Appl. Magn. Reson. (2008) 33, 57–71
DOI 10.1007/s00723-008-0056-1
Printed in The Netherlands

Applied Magnetic Resonance

Ferromagnetic Resonance Fine Structure of Dispersed Magnets: Physical Origin and Applications

O. N. Martyanov, S. N. Trukhan, and **V. F. Yudanov**

Boreskov Institute of Catalysis, Russian Academy of Sciences, Novosibirsk, Russian Federation

Received 30 September 2006; revised 30 October 2006

Abstract. An original approach is proposed to study the dipole–dipole interparticle interactions in dispersed magnets. It is the registration and analysis of the noiselike ferromagnetic resonance fine structure, which is caused by the magnetic dipole–dipole interaction between magnetic domains. The features of fine structure formation are discussed. The experimental examples of the possible applications of the fine structure method are given.

1 Introduction

A lot of spectroscopic techniques have been successfully applied to accumulate information on structure and properties of magnetic nanoparticle-based systems. Even though these methods provide data on the atomic level, it has not been possible so far to unravel all details necessary to establish features of the collective behavior of nanostructured dispersed magnets [1–4]. As a result, the search for new analytical tools with sufficient sensitivity is continuing.

It has long been recognized that small changes in the substance structure influence its magnetic properties drastically (see, for example, refs. 5 and 6). Therefore, monitoring magnetic properties of these systems could help to provide a deeper insight into magnetic properties of dispersed magnetic nanostructures. Electron spin resonance (ESR) spectroscopy (usually called ferromagnetic resonance (FMR) in the case of ferromagnetic systems) has proved to be a valuable tool for both magnetic powders and single crystals [7–9]. However, FMR, a useful source of information in many cases, is limited by strong inhomogeneous broadening arising from a random orientation of the anisotropic magnetic particles when studying dispersed magnets. New possibilities of the FMR technique may provide studying the unusually narrow lines observed against the broad adsorption spectra [10–12]. In the present work, an original approach is proposed to study the dipole–dipole interparticle interactions in dispersed magnets on the basis of the registration and analysis of the noiselike FMR fine structure (FS) [11]. It

is shown that registration and analysis of FMR FS can be used to obtain a unique information about granular and heterogeneous magnetic systems unavailable before. Some possible applications of the FMR FS are given in the last part of this work.

2 Physical Background of the FMR FS Method

During the investigation of the magnetic properties by ESR, a gradual sweep of the external magnetic field usually leads to a gradual change of the local magnetic fields. This leads to gradual changes of the microwave resonance absorption with the magnetic field sweep. However, for example, in the classic case of the magnetization of a uniaxial ferromagnetic isolated crystal, a magnetization jump may take place with a gradual magnetic field increase due to the well-known hysteresis behavior. It would lead to a stepwise change of the microwave resonance absorption if one could operate with a single nanoparticle. But even

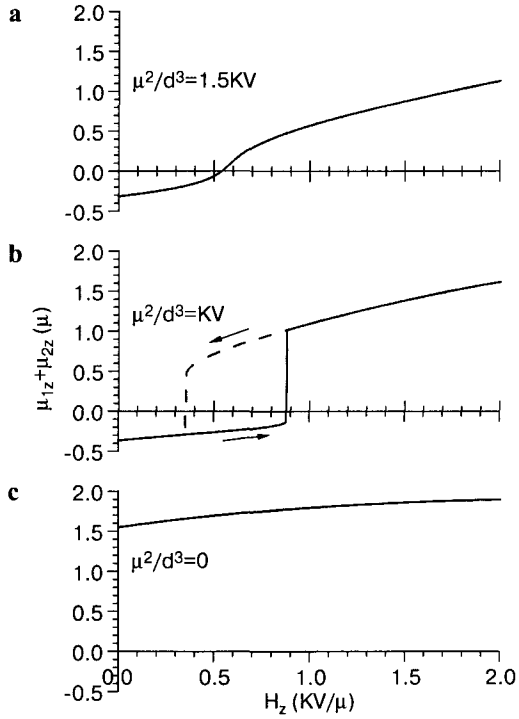

Fig. 1. Sum of magnetic moments projections of two interacting magnetic dipoles on the external magnetic field direction as a function of the external magnetic field in two-dimensional (2-D) case for the $\mu^2/d^3 = 1.5KV$ (**a**), $\mu^2/d^3 = KV$ (**b**), and $\mu^2/d^3 = 0$ (**c**). Here the angle between easy particle axes $\mathbf{n}_1$ and $\mathbf{n}_2$ and the external magnetic field **H** are $\theta_{n1} = 6.8°$ and $\theta_{n2} = 56.3°$, correspondingly for the $\boldsymbol{\mu}_1$ and $\boldsymbol{\mu}_2$. The angle between the vector of the mutual particles arrangement and external magnetic field is $\theta_d = 97.3°$.

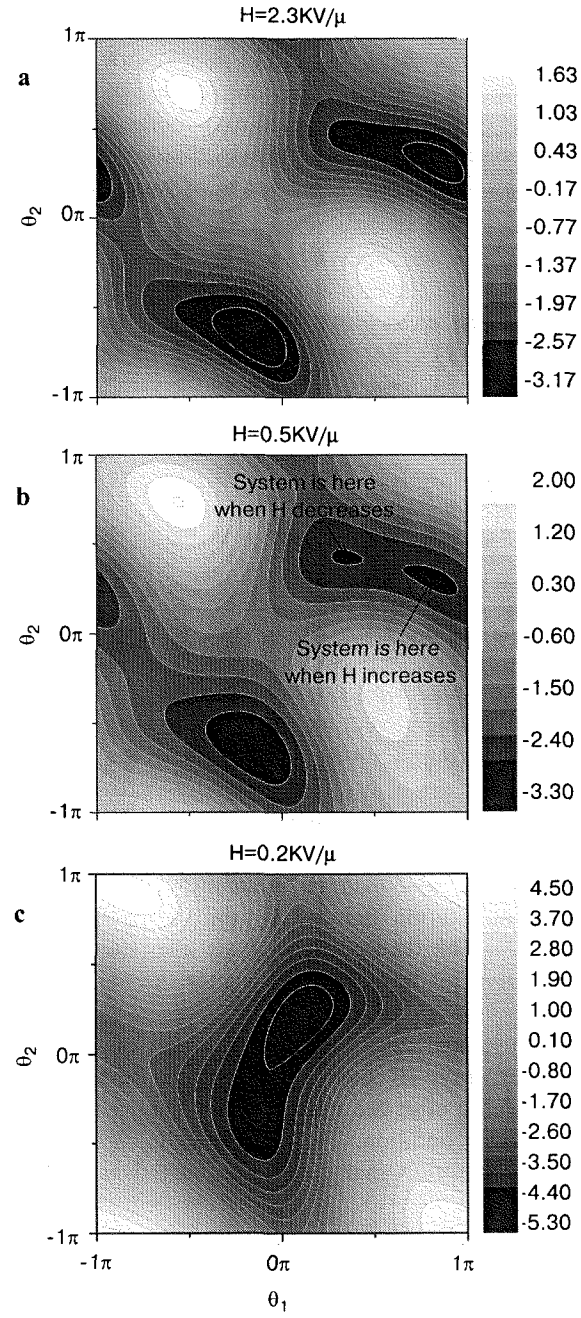

Fig. 2. Contour plot of energy of two interacting dipoles as a function of angles between particles magnetic moments ($\boldsymbol{\mu}_1$, $\boldsymbol{\mu}_2$) and an external magnetic field in 2-D case. $H = 2.3KV/\mu$ (**a**), $0.5KV/\mu$ (**b**), and $0.2KV/\mu$ (**c**). Here is $\mu^2/d^3 = KV$. The angle between easy particle axes $\mathbf{n}_1$ and $\mathbf{n}_2$ and the external magnetic field **H** as well as θ_d are the same as in Fig. 1.

in this case, the latter situation could take place in the FMR spectra only once, at the first scan. To repeat such a jump, the specimen needs to be placed in the oppositely directed magnetic field. In ref. 11 it was first shown using a simple two-particle model that the dipole–dipole interaction can lead to the magnetization jump upon changing the magnetic field magnitude but not its direction. The hysteresis occurs when the Zeeman, the dipole–dipole interaction and the effective anisotropy energies are of the same order of magnitude

$$E_{\mathrm{H}} \sim E_{\mathrm{d\text{-}d}} \sim E_{\mathrm{anis}}. \tag{1}$$

Here we calculated the energy of the two-particle system and correspondent magnetization curve (Fig. 1). The particles possess the axial effective anisotropy of both the geometric (anisotropy of shape) and crystallographic character. Besides the Zeeman energy, we took into account the dipole–dipole interaction between the particles. The energy of the system is

$$E = E_{\mathrm{anis}} + E_{\mathrm{d\text{-}d}} + E_{\mathrm{H}} = -\frac{KV}{\mu^2}\left[(\boldsymbol{\mu}_1\mathbf{n}_1)^2 + (\boldsymbol{\mu}_2\mathbf{n}_2)^2\right] + \frac{d^2\boldsymbol{\mu}_1\boldsymbol{\mu}_2 - 3(\mathbf{d}\boldsymbol{\mu}_1)(\mathbf{d}\boldsymbol{\mu}_2)}{d^5} - H(\boldsymbol{\mu}_1 + \boldsymbol{\mu}_2),$$

here K is the effective anisotropy constant, V is the volume of each particle, $\boldsymbol{\mu}_{1,2}$ are the magnetic moment vectors of the particles ($\mu = |\boldsymbol{\mu}_1| = |\boldsymbol{\mu}_2|$), $\mathbf{n}_{1,2}$ are the easy-axis magnetization directions, and $\mathbf{d}$ is the vector of their mutual arrangement.

The simulation showed that an increase of the dipole–dipole interaction leads to the appearance of a hysteresis entirely observed in the positive magnetic field (Fig. 1). The abrupt changes of magnetization projection correspond to the stepwise magnetic moment rotation induced by the disappearance of the local energy minimum (Fig. 2). The theoretical analysis also showed that the hysteresis position is very sensitive to the $\mathbf{n}_{1,2}$ and $\mathbf{d}$ vector orientation relative to the external magnetic field.

The magnetization jumps lead to stepwise changes of the local magnetic field for the particles under study. If one of the ferromagnetic particles has a resonance adsorption before or after the magnetization jumps it should lead to abrupt changes in its resonance condition. The latter results in a stepwise variation of the microwave field absorption that can be registered as the additional narrow line in the FMR spectrum.

3 FMR FS of Dispersed Magnets

In the dispersed system of interacting ferromagnetic particles, it is reasonable to expect the existence of multiple magnetization jumps that can be registered in FMR spectra as extra narrow lines (FS) against well-known wide absorption

signals. The important distinctive feature of this FS should be the reproducibility along with a strong orientation dependence. Figure 3 shows the result of the numerical simulation of magnetization jumps in randomly oriented dispersed magnets. The calculation was made by the summation of pairs of randomly oriented particles coupled in a dipole–dipole manner. Details and features of the numerical simulation will be discussed elsewhere. It appeared that FMR FS can occur with different parameters. It is sensitive to the geometry and size of the particles, as well as to their magnetic characteristics. The necessary condition for the hysteresis to occur is the same order of magnitude for competitive energy constituents. Of course, in a real dispersed system, the situation is more complicated. To reproduce the two-particle model better, one can dilute dispersed magnets and remove the agglomerates.

Indeed, the investigation of the model nonoriented granular magnets revealed the noiselike but strictly reproducible FS of the FMR spectra which was observed as a multitude of narrow lines of the two-order weaker intensity. The experimental spectra were registered on a Bruker EMX 3-cm spectrometer. The specimens were placed at the center of a rectangular TE_{102} cavity. The modulation frequency was 100 kHz. The temperature control system provided measurements in the 77–500 K range. The observed FS possesses all expected features, including a strong orientation dependence and dependence on the dipole–dipole interparticle interaction. Figure 4 shows an FMR spectrum of a γ-Fe_2O_3 powder obtained in the high-sensitivity conditions. There is an intense inhomogeneous broad signal usually observed in ferromagnets. However, against a broad background spectrum one can observe lines in the wide range of magnetic fields two orders of magnitude weaker and extremely sharp. With a single magnetic sweep, these lines are virtually lost in the noise and their reliable recording requires a digital accumulation. One can observe these lines while

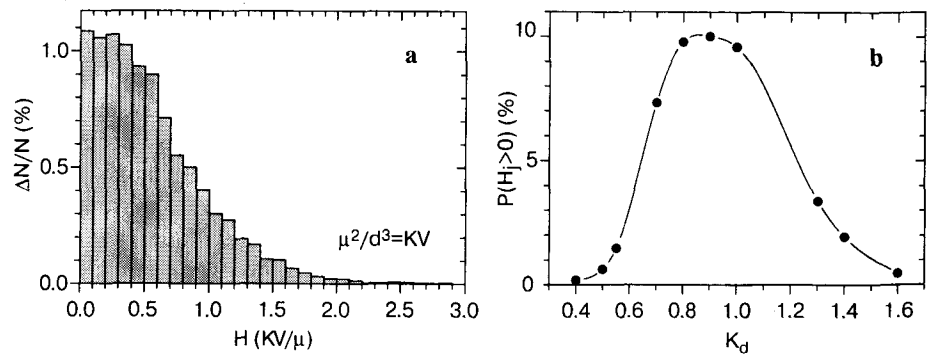

Fig. 3. **a** Probability of the magnetization jumps in the pairs of randomly oriented particles interacting in dipole–dipole manner. Here is $\mu^2/d^3 = KV$. The calculation was made using Monte Carlo simulation. Easy particle axes and the vector of the mutual particle arrangement are directed in a random way in 3-D space. **b** Fraction of the pairs for which the magnetization jumps can appear at $H > 0$ as a function of the value of the dipole–dipole interaction $K_d = (\mu^2/d^3)/(KV)$. At $\mu^2/d^3 = KV$ (**a**) this fraction is 9.6%.

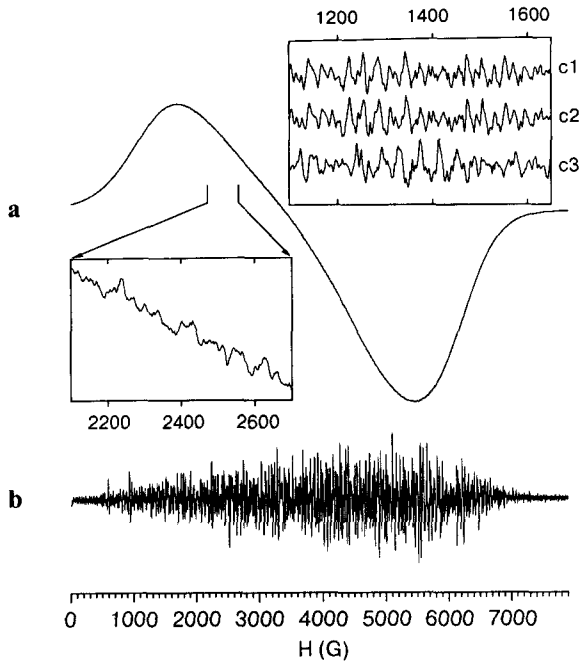

Fig. 4. FMR spectrum of γ-Fe_2O_3 powder in a paraffin matrix. **a** General view. **b** FS of the FMR spectrum after subtraction of the smooth component. According to the electron microscopy data, individual particles have an elongated shape with average size of about 0.1 μm. The content of γ-Fe_2O_3 is about 1 wt%. Curves c1 and c2 form a sequence of FS spectra recorded in the independent registration series, curve c3 denotes to the specimen rotated by 0.5° relative to curve c2.

looking carefully at the intensive broad spectrum, but to analyze the FS, it is convenient to eliminate the wide smooth component calculated by the removal of higher-than-given Fourier harmonics of the spectrum. It was checked that the procedure does not change the noiselike component. The spectra below are given after subtraction.

The observed spectra (Fig. 4) consist of a large number of lines that are rather narrow for a solid (~10 G). Along with the noiselike character these spectra are strictly reproducible (see inset, spectra c1 and c2) (Fig. 4). The change of registration conditions does not change the pattern over a long period of time. The changes of the magnetic field modulation frequency and amplitude (within the individual line width), the microwave power, the integration time constant and the field sweep rate leave the spectrum unchanged and allow the absorption pattern to be recorded invariable over indefinite periods. At the same time the reproduction of the noiselike spectra is observed at the one-way sweep direction only. The spectra shown in Fig. 4 correspond to the upward traces. As it was predicted, the spectra have a strong orientational dependence. An infinitesimal rotation of the specimen causes noticeable changes in the spectrum (spectrum c3 in the inset of Fig. 4). To analyze and compare FS, we used a correlation functional analysis.

It was checked that the experimental FS spectra of dispersed magnets are the sum of the adsorption jumps from different particles. FS can be observed only if the total number of narrow lines from different summable particles is inadequate to form a smooth contour [13, 14]. This may be realized in the powder if the lines originated from the magnetization jumps are narrow and strong enough. Indeed, it was shown that the FS spectra intensity increases as a square root of the value of the ferromagnetic phase. It means that FS in a powder is the result of incomplete averaging of lines from different particles.

FS is registered in all dispersed magnets checked, but with some differences. For example, the Ni powder specimen put in the cavity does not display any FS spectra. This is not surprising if one remembers the main condition for FS to appear – the same order of magnitude for the Zeeman, dipole–dipole and effective anisotropy energies. Ni has larger saturation magnetization as compared with that of the γ-Fe_2O_3, therefore, to observe FS it is necessary to dilute it in some nonmagnetic matrix to satisfy the condition Eq. (1). By the way, the reverse effect is observed for pressed ferromagnetic powders. We failed to reveal the FMR FS for pressed γ-Fe_2O_3 powders, while the regular FMR spectrum was the same.

As predicted, we revealed that the FS is considerably determined by the value of the magnetic interparticle interaction. The dilution and the uniform separation of the aggregated particles by ultrasonic dispersion in diamagnetic matrix lead to the concentration of lines in particular regions of the magnetic field (Fig. 5a). The same order is observed for different ferromagnetic powders, but at different magnetic field values, reflecting features of the dispersed specimen. These features were clarified after the consideration of the magnetization behavior of Ni dispersed in wax. Kittel et al. [15] showed experimen-

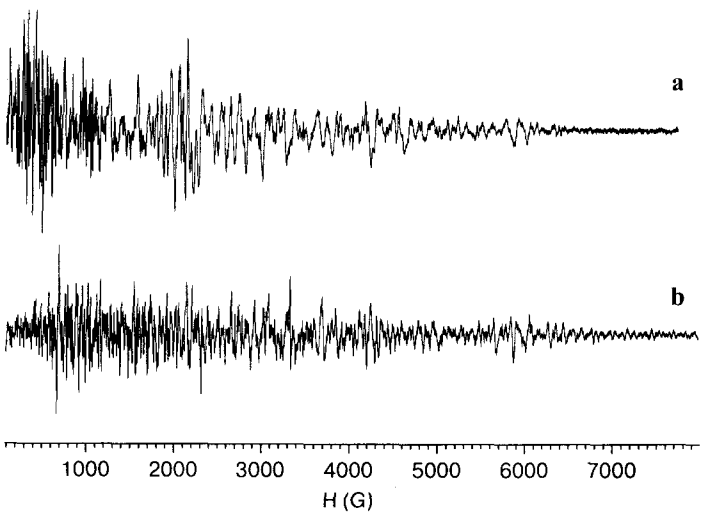

Fig. 5. FMR FS of Ni powder prepared by ultrasonic dispersion in a melted paraffin matrix. Temperatures of registration were 300 K (**a**) and 77 K (**b**). The content of Ni is about 1 wt%.

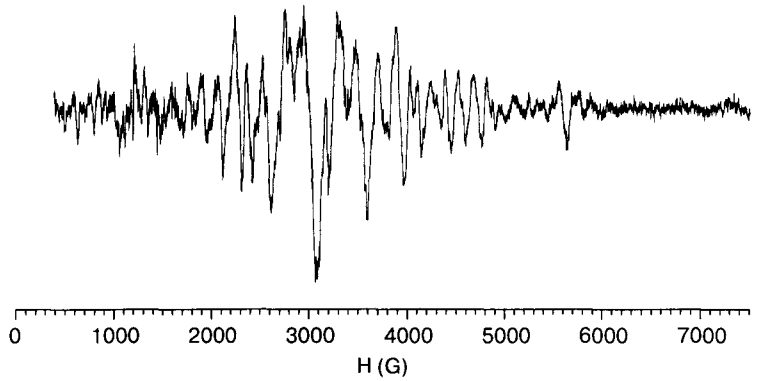

Fig. 6. FS of the FMR spectrum for Ni powder prepared by mechanic stirring in a paraffin matrix without ultrasonic dispersion. The content of Ni is about 1 wt%.

tally and theoretically that to magnetize an isolated particle it is necessary to overcome the self-demagnetization field equal to $2K/J$ and $4\pi J_s/3$ for single- and multidomain particles, respectively. Here K is the crystallographic anisotropy constant and J_s is the saturation magnetization. For the metal Ni, the corresponding values qualitatively coincide with FS intensity maxima [12]. So the low-field range is associated with the single-domain particles, while the multidomain particles can cause the high-field range. The absorption lines in the highest fields can be attributed to magnetization of the largest agglomerated particles with a high demagnetization factor. This interpretation was checked experimentally. The low-field part of FS is quite sensitive to the temperature because of K. So while the temperature decreases, the low-field part reversibly moves to the higher magnetic field, leading to a mixing of the previously separated regions (Fig. 5b).

The preparation of the Ni-dispersed specimen (Fig. 5a) includes ultrasonic dispersion, resulting (according to electron microscopy) in an increase of the number of small particles. If the Ni powder is stirred mechanically without ultrasonic dispersion, the number of small particles is sufficiently small. One can see that in this case (Fig. 6) the spectrum is free of the low-field part, which is formed by the smallest particles. This is additional evidence of the FS connection with magnetization in dispersed magnets.

Thus, FMS FS is a concurrent and essential property of dispersed magnets. The observed spectra carry complex information about the geometric and magnetic properties of particular powder particles and the interparticle interaction between them.

4 Application of the FS Approach

It is difficult to predict all possible areas of the FS phenomenon application. Anyway, the registration and analysis of FS can be used as a new tool for investi-

gation and characterization of different nanostructured magnetic dispersed systems. Figure 7 shows the FMR FS observed in the system consisting of oriented magnetic particles. The needle-shaped γ-Fe_2O_3 particles are aligned along their easy magnetization axis in the thin layer. One can see that the range of FS is narrower when the magnetic field is perpendicular to the film plane and the easy axis of magnetic particles and it is observed in higher magnetic field (Fig. 7, curve 2b) as compared with the parallel situation (Fig. 7, curve 1b) or randomly oriented powder (Fig. 4). This can be explained by the suppression of particle magnetic moments by the large film shape anisotropy in the plane. Therefore, when the magnetic field is perpendicular to the film plane, most of the particle magnetic moments are also perpendicular to the external magnetic field. In this case the resonance condition due to the film shape demagnetization factor leads to the FS observation in the narrow range of high magnetic fields. Thus, the analysis of the magnetic field values where FS is observable gives a unique possibility to estimate the degree and quality of the particle orientation in the dispersed system.

FS was registered in the high-sensitivity condition in different systems: oxides, polymers and zeolites. It appeared that FS was caused by ferromagnetic impurities in all these systems. Figure 8 demonstrates an extreme example of this situation [16]. Spectra of the empty ESR Bruker EMX spectrometer cav-

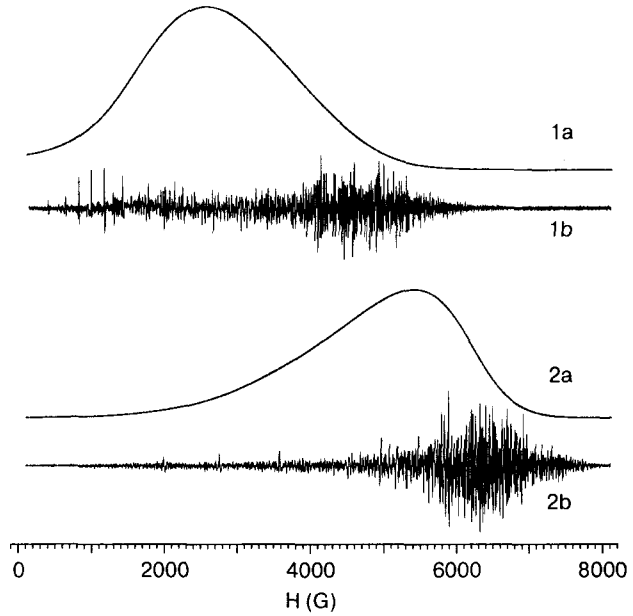

Fig. 7. Integral FMR absorption spectra (curves 1a and 2a) and their FS (curves 1b and 2b) that are observed in magnetically oriented systems of needle-shaped γ-Fe_2O_3 particles (length is about 0.5 μm) dispersed in the thin film. Particle easy direction lies in the plane of the film: magnetic field is parallel to the easy direction of magnetic particles (top) and perpendicular to the film plane and easy direction of magnetic particles (bottom).

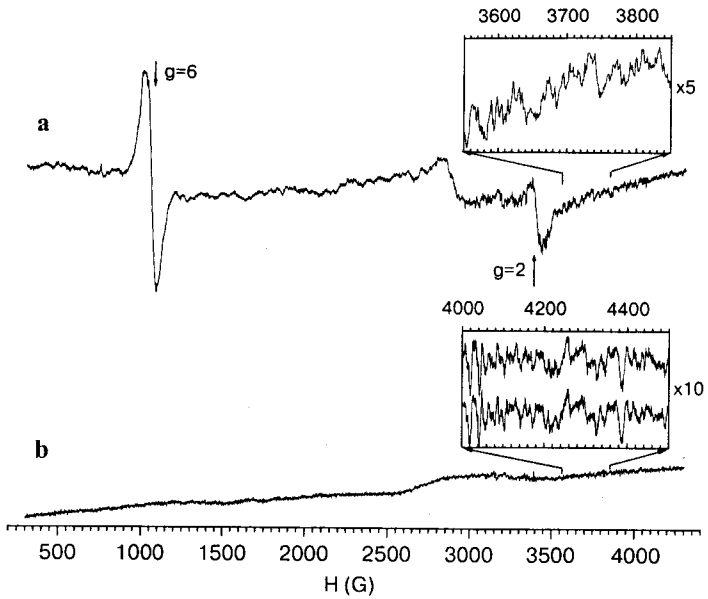

Fig. 8. Inherent spectrum of empty microwave cavity of Bruker EMX ESR spectrometer before rinsing (**a**) and after multiple rinsing (**b**).

ity are shown. Note that the intensity of these spectra is extremely small in comparison with the intensity of the signals usually investigated by ESR and even FS FMR spectra shown above. Spectra in Fig. 8 are obtained by the digital accumulation of more than 100 scans. Signals that can be distinguished in Fig. 8a are probably due to the presence of dust on the inner cavity wall. Along with these signals one can observe the weaker but reproducible noiselike FS. After repeated cavity rinsing the intensity of the FS decreased by a factor of no more than 3–5, while broad signals almost disappear (Fig. 8b). Thus, the FS of the uncontrolled ferromagnetic impurities in the cavity material limits the real sensitivity of present-day ESR spectrometers and the FMR FS approach can be used to monitor the presence of usually uncontrolled ferromagnetic impurities.

The FMR FS approach appeared to be productive in the investigation of magnetic inhomogeneities in doped manganites demonstrating a colossal magnetoresistance (CMR) effect. Spatial separation of the magnetic phases in manganites [17, 18] was proposed to explain CMR phenomena [19, 20]. Despite the experimental evidence of the spatial magnetic phase separation [21–25], a problem of such regions remains understudied. While the small-angle neutron scattering points to the nanometer size of ferromagnetic clusters [21, 24, 25], high-resolution electron microscopy advocates for a much larger scale of the spatial phase separation [22]. As FMR FS is the concurrent feature of dispersed magnets it can be registered even in a single crystal because of spatially separated ferromagnetic domains. Indeed, the FMR FS approach appeared to be very sensitive to the temperature behavior of magnetic phase separation and correlates with magnetotransport properties.

We investigated $La_{0.7}Pb_{0.3}MnO_3$ single crystals grown by spontaneous crystallization from solution in melt [26]. The initially prepared crystals are cubes with a size of 4 by 4 by 4 mm and a shiny black surface. X-ray data show that the crystals are monophasic and have a perovskite-like rhombohedral structure with the *R3c* space group and the unit cell parameters $a = 0.552370$ nm and $c = 1.340233$ nm. Magnetostatic study in low magnetic fields on a vibrating sample magnetometer gave the temperature of transition to the ferromagnetic state $T_c = 357$ K. The spectra were registered on a Bruker EMX spectrometer. Magnetic resonance studies were carried out on well-polished spherical specimens (~0.5 mm) to eliminate the shape anisotropy factor.

Figure 9 shows the FMR absorption spectrum of $La_{0.7}Pb_{0.3}MnO_3$ single crystal. The spectrum is typical for a magnetic inhomogeneous system and contains two absorption lines which may be associated with ferro- and paramagnetic phases occurring in a manganite single crystal [27]. However, rather weak and narrow absorption lines are revealed against the background of the wide FMR spectrum (Fig. 9b). Spectral characteristics of the observed narrow lines, the strong orientation dependence along with the strict reproducibility allow these lines to be assigned to the noiselike FMR FS revealed and investigated in dis-

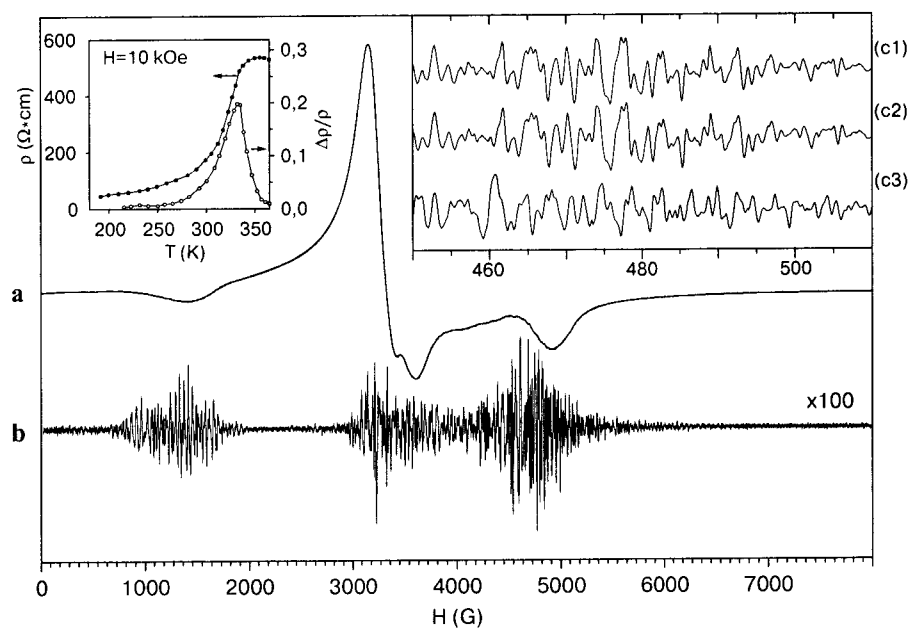

Fig. 9. FMR spectrum of $La_{0.7}Pb_{0.3}MnO_3$ spherical single crystal. **a** General view. **b** FMR FS obtained after subtraction of the smooth background component. In the inset, curves c1 and c2 form a sequence of FMR FS spectra obtained in independent registration series at unchangeable specimen position in the spectrometer cavity, curve c3 denotes to the specimen turned by 1°, $T_{reg} = 296$ K.

persed magnets [12]. At room temperature, the FS of $La_{0.7}Pb_{0.3}MnO_3$ single crystal is observed over two regions of the magnetic field, from 600 to 2000 G with the maximum at 1400 G and from 2700 to 6000 G. With a temperature decrease, the two regions shift towards each other and at 105 K the FS is observed over one region of 2000–6500 G. The FMR FS is observed in a single crystal. It allows us to conclude that the manganite single crystal under study contains spatially separated ferromagnetic regions coupled by the dipole–dipole interaction. It should be noted that when studying lanthanum manganite powders with the FMR method, some authors [28, 29] encountered a manifestation of the FMR FS by registering the extra narrow lines against a background of the wide structureless signal. However, the FMR FS of the dispersed specimen is complicated because of the dipole–dipole interaction between individual powder particles; therefore, the magnetic phase separation has to be studied only in single crystals.

Figure 10 shows the FMR FS spectra of the $La_{0.7}Pb_{0.3}MnO_3$ single crystal in the vicinity of the Curie point. As the temperature increases, the low-field part of the FMR FS spectrum shifts towards the lower magnetic fields. Such behavior corroborates Eq. (1): the size of ferromagnetic domains and the crystallographic anisotropy constant decrease with the temperature growth resulting in the decrease of E_{d-d} and E_{anis}; and condition Eq. (1) is fulfilled for the lower magnetic field. The FMR FS intensity decreases as the Curie point is approached. At 330 K, the low-field part of the FS disappears, while the high-field lines are registered at higher (up to 340 K) temperatures. This can be interpreted as follows: the smallest ferromagnetic domains disappear first, while the large-scale

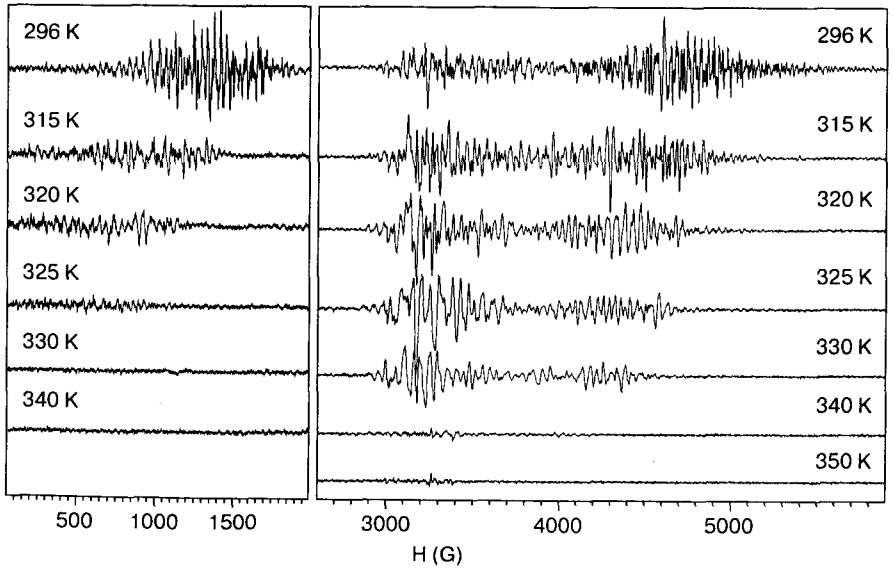

Fig. 10. Sequence of the FMR FS spectra of $La_{0.7}Pb_{0.3}MnO_3$ single crystal at various temperatures of the specimen.

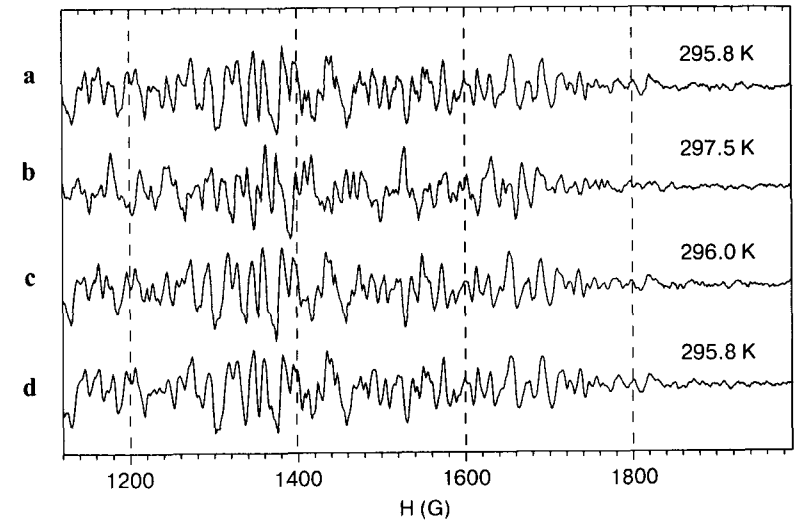

Fig. 11. FMR FS of the $La_{0.7}Pb_{0.3}MnO_3$ single crystal at various temperatures of the specimen. The temperature stability and accuracy of its determination was better than 0.1 K.

ferromagnetic dispersity remains practically up to the Curie temperature. The FS disappears totally at T_c when the transition of crystal to the homogeneous paramagnetic state takes place. It is interesting to note that the FS intensity drops at $T \sim 325$–335 K at the maximum value of the magnetoresistance (inset in Fig. 10), when the percolation of ferromagnetic domains takes place.

Despite the high sensitivity to the specimen temperature it was experimentally demonstrated that FS is temperature-reversible. Figure 11 shows the FMR FS spectra obtained with the temperatures that differ by fractions of a degree. The similarity of the spectra was estimated by the cross-correlation function. One can see that with the temperature increase by 1.7 K, the spectrum essentially changes (Fig. 11a and b). When the temperature returns to its original value, the FMR FS returns to its original state (compare Fig. 11a and d). Thus, the spatial distribution of magnetic phases in the single crystal monitored by FS is temperature-reversible.

5 Conclusion

The FMR FS approach at some points in fact increases the sensitivity and resolution of the FMR technique and can provide new information about magnetic characteristics of dispersed magnets and magnetization inside them. It also provides a unique possibility to measure directly the magnetic interparticle interactions in different dispersed systems.

The results obtained for manganites demonstrated the capabilities of the FMR FS to study the magnetic phase separation phenomenon. The observation of FMR

FS corroborates with the concept of the spatial magnetic phase separation in manganite single crystals. The FMR FS is proved to be very sensitive to the temperature and geometry of magnetic phase separation in manganite single crystals. It is shown that the spatial distribution of magnetic phases in the single crystal monitored by FMR FS is temperature-reversible. These data enabled the conclusion that the development of the FMR FS approach can be a new original tool to study features of the system with the magnetic phase separation phenomenon.

Acknowledgments

We are grateful to Yu. N. Molin who had supported this work at very first stage, N. V. Volkov for the manganites preparation. This research was supported by grants of the President of the Russian Federation MK-3310.2005.3 and the youth grant of the Siberian Branch of the Russian Academy of Sciences (2006). We thank also the Russian Science Support Foundation.

References

1. Held, G.A., Grinstein, G., Doyle, H., Sun, S., Murray, C.B.: Phys. Rev. B **64**, 012408–012412 (2001)
2. Yamamoto, T.A., Tanaka, M., Misaka, Y., Nakagawa, T., Nakayama, T., Niihara, K., Namazava, T.: Scr. Mater. **46**, 89–94 (2002)
3. Spasova, M., Wiedwald, U., Ramchal, R., Farle, M., Hilgendorff, M., Giersig, M.: J. Magn. Magn. Mater. **240**, 40–43 (2002)
4. Dennis, C.L., Borges, R.P., Buda, L.D., Ebels, U., Gregg, J.F., Hehn, M., Jouguelet, E., Ounadjela, K., Petej, I., Prejbeanu, I.L., Thornton, M.J.: J. Phys.: Condens. Matter **14**, R1175–R1262 (2002)
5. Li, S.P., Lew, W.S., Bland, J.A.C., Lopez-Diaz, L., Vaz, C.A.F., Natali, M., Chen, Y.: Phys. Rev. Lett. **88**, 087202–087206 (2002)
6. Sander, D.: Rep. Prog. Phys. **62**, 809–858 (1999)
7. Pinarello, G., Pisani, C., D'Ercole, A., Chiesa, M., Paganini, M.C., Giamello, E., Diwald, O.: Surf. Sci. **494**, 95–110 (2001)
8. Farle, M.: Rep. Prog. Phys. **61**, 755–826 (1998)
9. Schlienz, H., Beckendorf, M., Katter, U.J., Risse, T., Freund, H.-J.: Phys. Rev. Lett. **74**, 761–764 (1995)
10. Yudanov, V.F., Mart'yanov, O.N.: Dokl. Phys. Chem. **357**, 652–656 (1997)
11. Yudanov, V.F., Martyanov, O.N., Molin, Y.N.: Chem. Phys. Lett. **284**, 435–439 (1998)
12. Martyanov, O.N., Lee, R.N., Yudanov, V.F.: J. Magn. Magn. Mater. **267**, 13–18 (2003)
13. Mart'yanov, O.N., Yudanov, V.F.: J. Struct. Chem. **40**, 878–893 (1999)
14. Yulikov, M.M., Mart'yanov, O.N., Yudanov, V.F.: J. Struct. Chem. **41**, 883–887 (2000)
15. Kittel, C., Galt, J.L., Campbell, W.E.: Phys. Rev. **77**, 725 (1950)
16. Mart'yanov, O.N., Yudanov, V.F.: Instrum. Exp. Tech. **42**, 69–73 (1999)
17. Moreo, A., Yunoki, S., Dagotto, E.: Science **283**, 2034–2040 (1999)
18. Khomskii, D.: Physica B **280**, 325–330 (2000)
19. Coey, J.M.D., Viret, M., von Molnar, S.: Adv. Phys. **48**, 167–293 (1999)
20. Tokura Y.: Colossal Magnetoresistive Oxides. Gordon and Breach Science, New York (1998)
21. De Teresa, J.M., Ibarra, M.R., Algarabel, P.A., Ritter, C., Marquina, C., Blasco, J., Garcia, J., Moral, A., Arnold, Z.: Nature **386**, 256–259 (1997)
22. Uehara, M., Mori, S., Chen, C.H., Cheong, S.-W.: Nature **399**, 560–562 (1999)

23. Simon, C., Mercone, S., Guiblin, N., Martin, C.: Phys. Rev. Lett. **89**, 207202–207206 (2002)
24. Radaelli, P.G., Ibberson, R.M., Argyriou, D.N., Casalta, H., Andersen, K.H., Cheong, S.-W., Mitchell, J.F.: Phys. Rev. B **63**, 172419–172423 (2001)
25. Lynn, J.W., Erwin, R.W., Borchers, J.A., Huang, Q., Santoro, A., Peng, J.L., Li, Z.V.: Phys. Rev. Lett. **76**, 4046–4049 (1996)
26. Volkov, N.V., Petrakovskii, G.A., Sablina, K.A., Koval, S.V.: Fiz. Tverd. Tela (St. Petersburg) **41**, 1842–1849 (1999)
27. Petrakovski, G.A., Volkov, N.V., Vasil'ev, V.N., Sablina, K.A.: JETP Lett. **71**, 144–147 (2000)
28. Ramos, C.A., Causa, M.T., Tovar, M., Obradors, X., Pinol, S.: J. Magn. Magn. Mater. **177–181**, 867–868 (1998)
29. Shames, A.I., Rozenberg, E., McCarroll, W.H., Greenblatt, M., Gorodetsky, G.: Phys. Rev. B **64**, 172401–172405 (2001)

Authors' address: Oleg N. Martyanov, Boreskov Institute of Catalysis, Russian Academy of Sciences, Prospekt Akademika Lavrentieva 5, Novosibirsk 630090, Russian Federation
E-mail: oleg@catalysis.ru